

# The $\nu_4$ bands at 11 $\mu\text{m}$ : linelists for the Trans- and Cis- conformer forms of nitrous acid (HONO) in the 2019 version of the GEISA database

Molecular Physics, DOI: 10.1080/00268976.2021.1951860

R. Armante<sup>a</sup>, A. Perrin<sup>a</sup>, F. KwabiaTchana<sup>b</sup>, L. Manceron<sup>c</sup>,



<sup>a</sup>Laboratoire de Météorologie Dynamique/IPSL, UMR CNRS 8539, Ecole Polytechnique, Université Paris-Saclay, Palaiseau Cedex, France;

<sup>b</sup>Laboratoire Inter-Universitaire des Systèmes Atmosphériques (LISA), UMR 7583, CNRS et Universités Paris Est et Paris Diderot, Institut Paul Simon Laplace, 94010 Créteil, France

<sup>c</sup>Ligne AILES, Synchrotron SOLEIL, L'Orme des Merisiers, St-Aubin BP48, 91192 Gif-sur-Yvette Cedex, France and MONARIS UMR 8233, CNRS-UPMC 75005, Paris, France.

(e-mail: [Raymond.armante@lmd.ipsl.fr](mailto:Raymond.armante@lmd.ipsl.fr), [Agnes.Perrin@lmd.ipsl.fr](mailto:Agnes.Perrin@lmd.ipsl.fr),

Using parameters of line positions and line intensities existing in the literature for the Trans- and Cis- conformer forms of nitrous acid (HONO), we generated, for the first time, a linelist of positions, intensities, and line shape parameters for the  $\nu_4$  bands of nitrous acid located at 790.117 and 851.943  $\text{cm}^{-1}$  for the Trans- and Cis- conformers, respectively. A validation of this linelist was performed using spectra recorded by the IASI (Interferometre Atmosphérique de Sondage Infrarouge) satellite instrument in February 2009 during the (rather) exceptional conditions of the large Australian bush fires. This list, which is now included in the 2020 version of the GEISA database (<https://geisa.aeris-data.fr/>), is of potential interest for the IASI-NG (Infrared Atmospheric Sounding Interferometer . New Generation) instrument which will be launched on board the METOP-SG satellite.

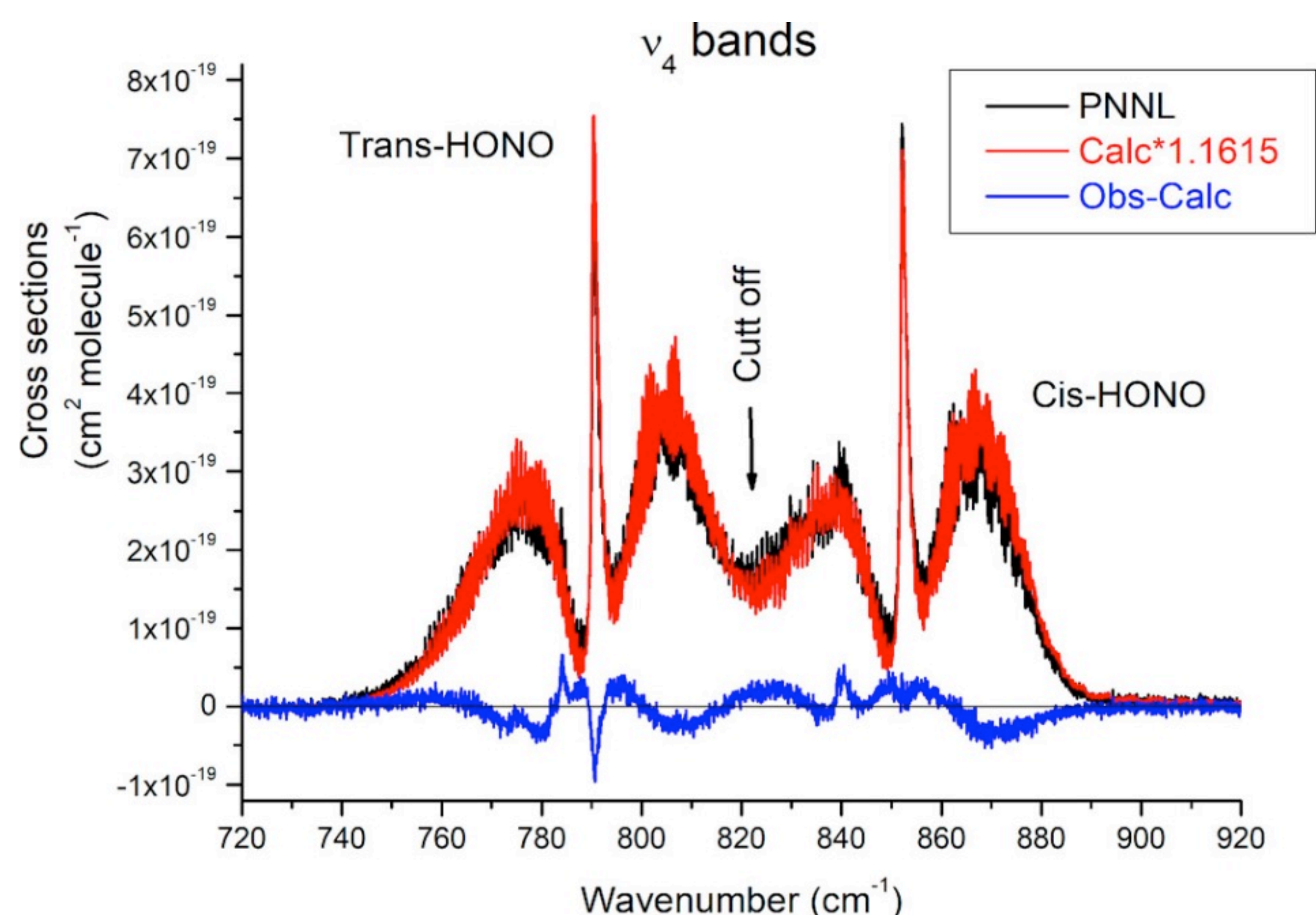


Figure 1. Comparison between the PNNL cross-sections and the results of the present computation at  $T = 296\text{ K}$  (HONO diluted in an atmosphere of nitrogen and for  $\gamma_{\text{Air}} = 0.1\text{ cm}^2/\text{Atm}$ ). For an easier comparison, the calculated cross-sections (this work) are multiplied by the mean (Trans- and Cis-HONO) vibrational partition function  $Z_{\text{Vib}}(296\text{ K}) = 1.1615$  to account for the hot bands contributions.

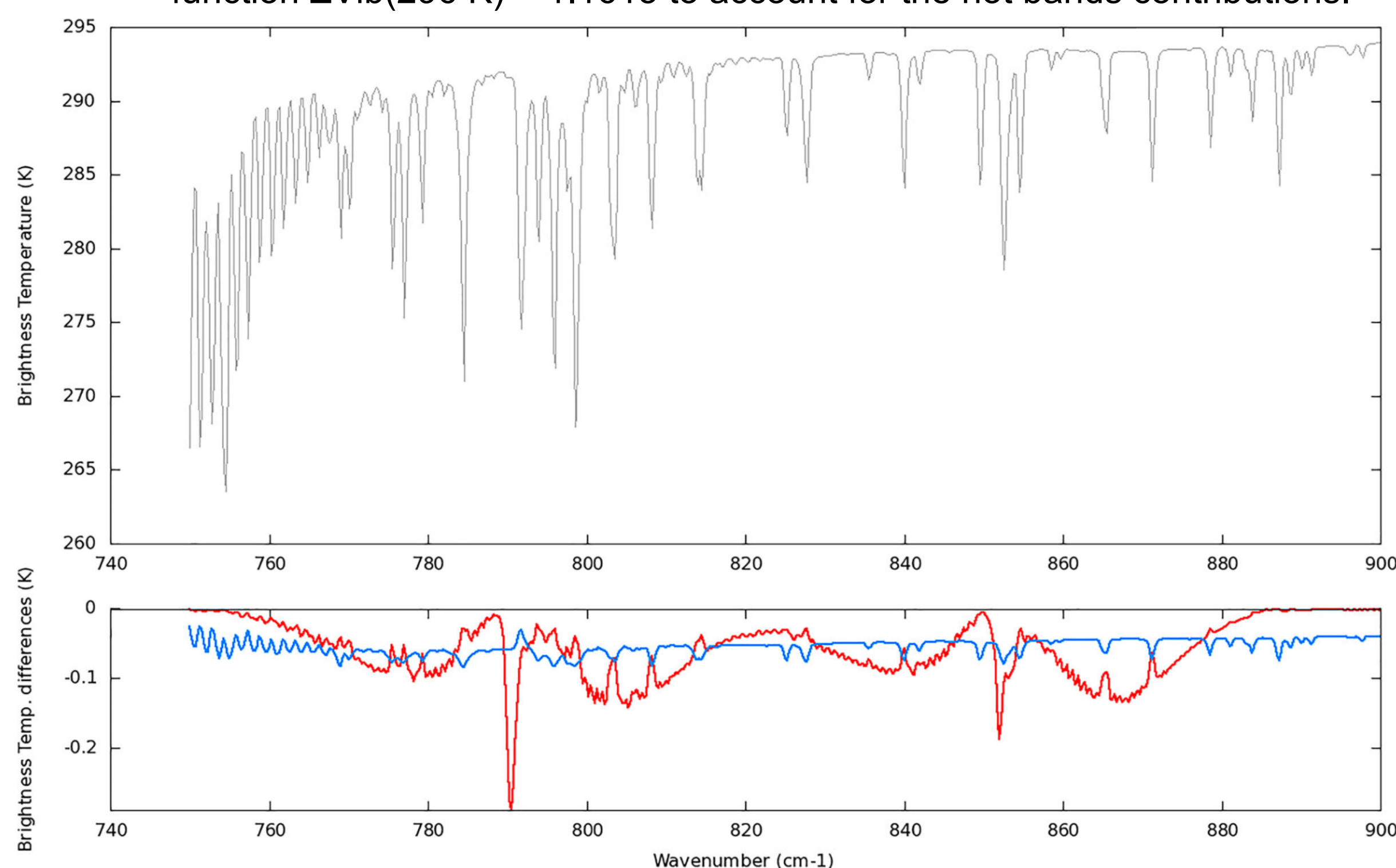


Figure 3. Simulation in brightness temperature (K) of a HONO signature on IASI spectra. This computation was performed for a total content of HONO of 1.03 ppbv and for a mean tropical atmosphere and using the 4A/OP radiative transfer code. On the top is represented the spectra with in brightness temperature. Below is represented respectively, in red the Brightness Temperature difference (Brightness Temp. differences) in K between the two simulations and in blue the sensitivity to a variation of 1% of water vapour, the main pollutant in the spectral region of HONO.

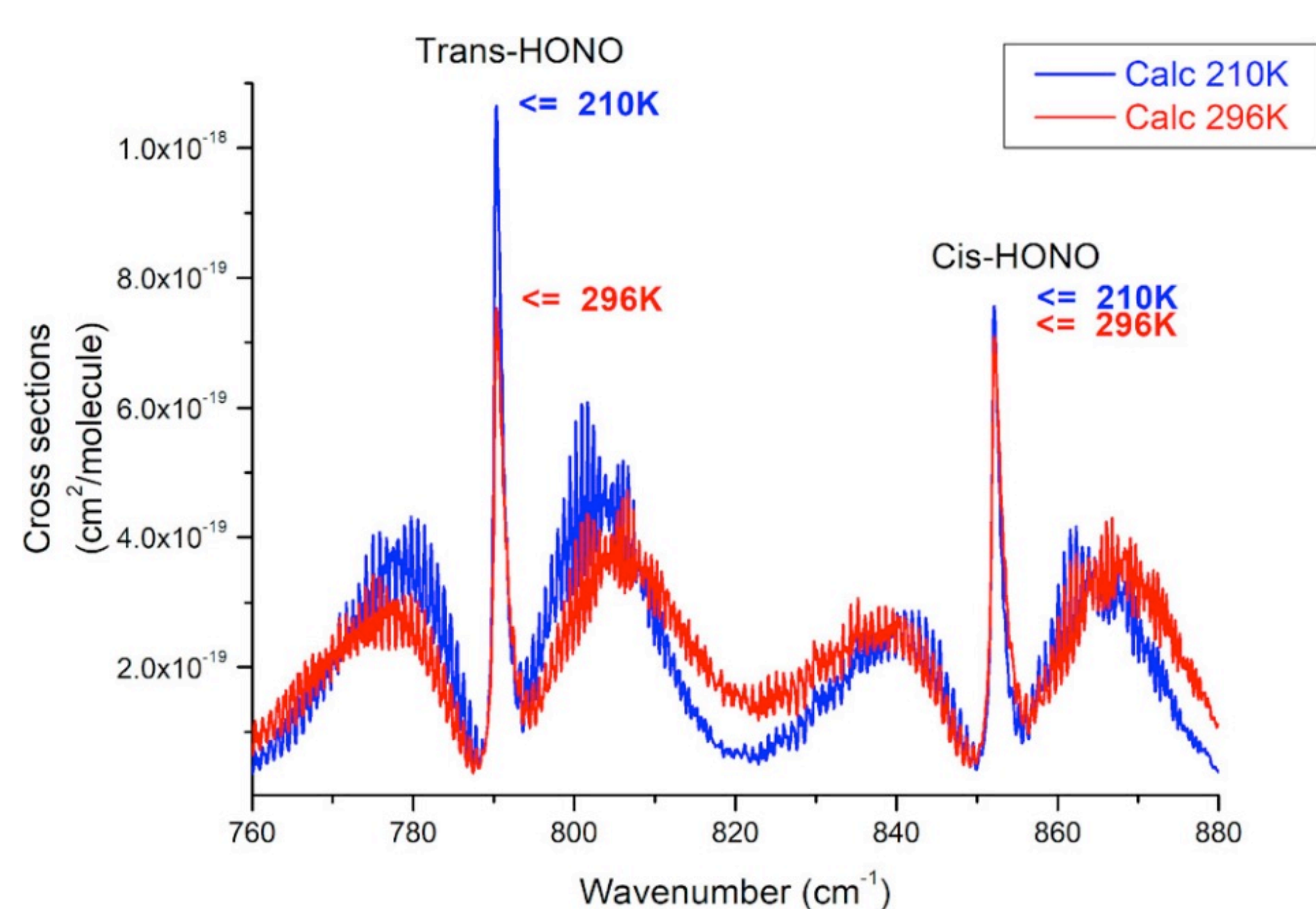


Figure 2. Computed cross-sections calculated using the present linelist for the  $\nu_4$  bands of Trans- and Cis-HONO at  $T = 296\text{ K}$  and at  $T = 210\text{ K}$ , respectively. These calculations were performed for the same HONO concentration than in Figure 1. It is clear that the relative contribution of the Cis- form to the HONO signature at 11  $\mu\text{m}$  relative to the Trans- one is significantly weaker at low temperatures.

**Table 3.** Results of the present line intensity and position computation at 296 K.

Conformer	Nb	Sig_min	Sig_max	Int_Max <sup>a</sup>	Total_Int <sup>a</sup>
Trans-HONO	7621	724.39	838.57	0.166	<sup>Trans</sup> Int( $\nu_4, T$ ) = 1.211
Cis-HONO	18420	722.53	996.28	0.148	<sup>Cis</sup> Int( $\nu_4, T$ ) = 1.241
Total	26041				Int( $\nu_4, T$ ) = 2.452
All lines (Trans- and Cis-)		Sigma < 820 $\text{cm}^{-1}$		Sigma > 820 $\text{cm}^{-1}$	11 $\mu\text{m}$
Sum of the individual intensities <sup>a</sup>		$\sigma < 820$ Int( $\nu_4, 296\text{ K}$ ) <sup>a</sup>		$\sigma > 820$ Int( $\nu_4, 296\text{ K}$ ) <sup>a</sup>	Int( $\nu_4, 296\text{ K}$ ) <sup>a</sup>
Calculation (This work)		1.25		1.20	2.45
Integrated band intensities <sup>b</sup>		$\sigma < 820$ S(296 K) <sup>a</sup>		$\sigma > 820$ S(296 K) <sup>a</sup>	S(11 $\mu\text{m}, 296\text{ K}$ ) <sup>a</sup>
Computed (this work) <sup>b,c</sup>		1.45		1.40	2.85
PNNL <sup>d</sup> [10]		1.44		1.40	2.84

Notes: Nb: number of lines; Sig\_Min, Sig\_Max; minimum and maximum sigma values (in  $\text{cm}^{-1}$ ).

<sup>a</sup>All intensities are given in  $10^{-17}\text{ cm}^{-1}/(\text{molecule cm}^{-2})$  at 296 K.

<sup>b</sup>Total Int:  $\text{Trans}^{\text{Int}}(\nu_4, T)$ ,  $\text{Cis}^{\text{Int}}(\nu_4, T)$  and  $\text{Int}(\nu_4, T) = \text{Trans}^{\text{Int}}(\nu_4, T) + \text{Cis}^{\text{Int}}(\nu_4, T)$ : sum of the individual intensities for the Trans- and Cis- isomers and for both isomers, respectively.

Int\_Max: Maximum intensity. The intensity threshold limit is  $\text{Int\_Min} = 0.5 \times 10^{-24}\text{ cm}^{-1}/(\text{molecule cm}^{-2})$ .

Total Int: sum of the individual intensities for the Trans and Cis forms,  $\text{Trans}^{\text{Int}}(\nu_4, T = 296\text{ K})$  and  $\text{Cis}^{\text{Int}}(\nu_4, T = 296\text{ K})$ , respectively.

Sigma < 820  $\text{cm}^{-1}$ , Sigma > 820  $\text{cm}^{-1}$ , and 11  $\mu\text{m}$ : sum of the individual line intensities (Int( $\nu_4, 296\text{ K}$ )) or integrated band intensities (S(11  $\mu\text{m}, 296\text{ K}$ )) in the 720–820  $\text{cm}^{-1}$ , 820–1000  $\text{cm}^{-1}$  and in the full 11  $\mu\text{m}$  region (720–1000  $\text{cm}^{-1}$ ), respectively. The 820  $\text{cm}^{-1}$  cut-off is defined in Equation (8).

<sup>c</sup>The computed integrated band intensities are deduced from  $\sigma < 820$ Int( $\nu_4, 296\text{ K}$ ),  $\sigma > 820$ Int( $\nu_4, 296\text{ K}$ ), and Int( $\nu_4, 296\text{ K}$ ) by a multiplication by  $Z_{\text{Vib}}(296\text{ K}) = 1.1615$  (see Equation (23)).

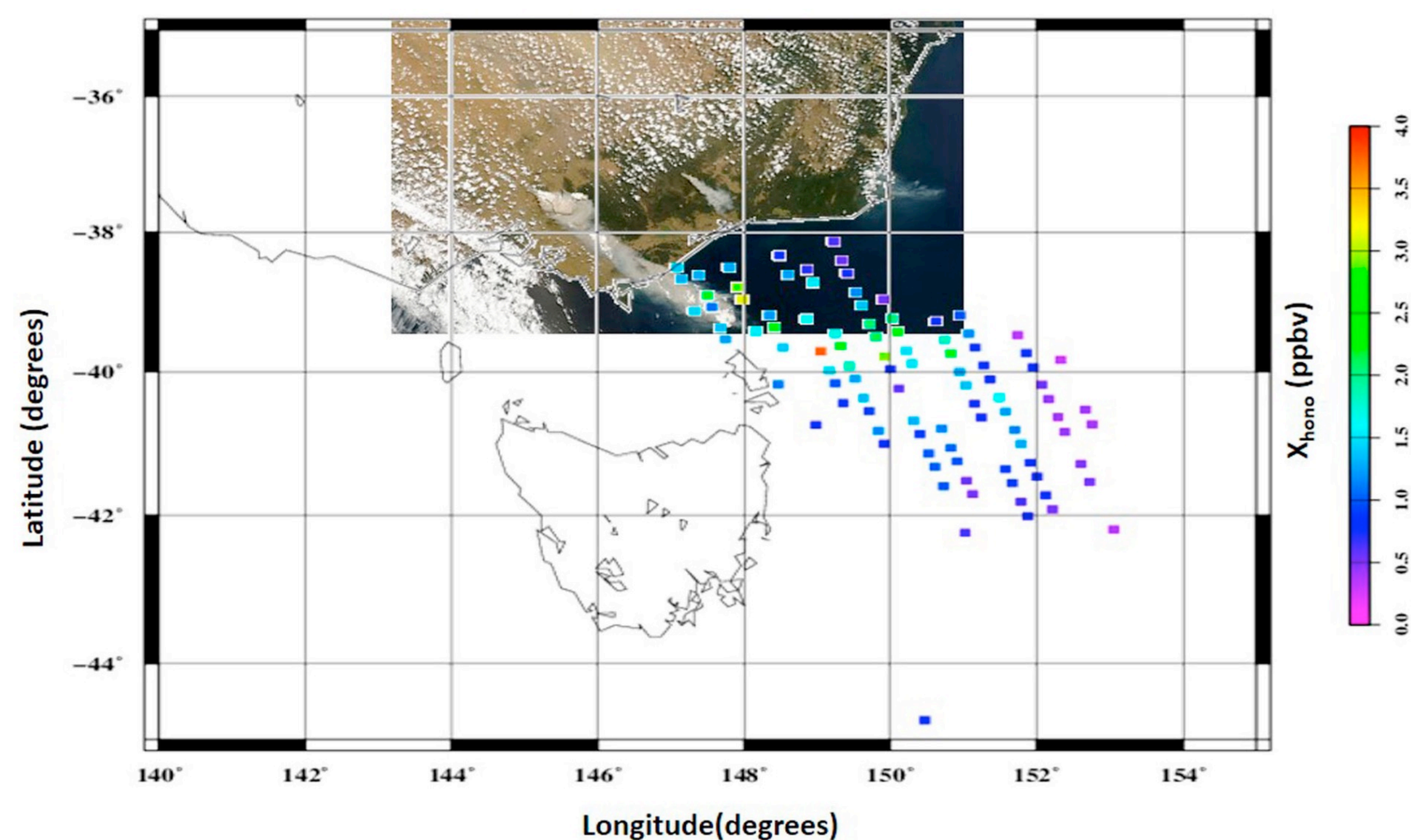


Figure 4. True colour imagery from the US MODIS Aqua satellite passes around 04 UTC (7 February, 3 PM EDT) on Saturday 7 February 2009 showing the smoke plumes from fires, including the dense cloud column ascending to high altitudes from the Kilmore fire (Image courtesy of MODIS Rapid Response Project at NASA/GSFC). The  $X^{\text{HONO}}$  inversions points (coloured squares) performed for the IASI instrument (9:30 PM) on the same day are over plotted in the range 0–4 ppbv and for a zone in latitude and longitude over the south of Australia and the Tasmania island, respectively.

## References:

- [6] L. Clarisse, Y. R'Honi, P.-F. Coheur, D. Hurtmans and C. Clerbaux, Geoph. Res. Lett. **38**, L10802 (2011).
- [7] C. Clerbaux, A. Boynard, L. Clarisse, M. George, J. Hadji-Lazaro, H. Herbin, D. Hurtmans, M. Pommier, A. Razavi, S. Turquety, C. Wespes and P.-F. Coheur, A.C.P. **9**, 6041–6054 (2009).
- [8] N. Jacquinet-Husson, R. Armante, N.A. Scott, A. Chedin, *et al.* JQSRT **327**, 31–72 (2016); T. Delahaye, R. Armante, N.A. Scott, N. Jacquinet-Husson, A. Chedin, *et al.* J. Mol. Spectrosc. **380**, 2021
- [9] I. Gordon *et al.* JQSRT **203**, 3–69 (2017); JQSRT **277** (2022)
- [10] S. Sharpe, T. Johnson, R. Sams, P. Chu, G. Rhoderick and P. Johnson, Appl. Spectrosc. **58**, 1452 (2004).
- [11] R. Kagann and A. Maki, JQSRT **30**, 37–44 (1983).
- [12] I. Kleiner, J.-M. Guilmet, M. Carleer and M. Herman, J. Mol. Spectrosc. **149**, 341–347 (1991).
- [13] A. Dehayem-Kamadjeu, O. Pirali, J. Orphal, I. Kleiner and P.-M. Flaud, J. Mol. Spectrosc. **234**, 182–189 (2005).
- [24] V. Sironneau, J.-M. Flaud, J. Orphal, I. Kleiner and P. Chelin, J. Mol. Spectrosc. **259**, 100–104 (2010).

The authors thank the AERIS atmospheric and data pole and the CNES French space agency to make available the IASI level 1 data. Work also supported by the French National programme ANR (ANR-19-CE29-0013) 'QUASARS'.